DØ Note 4545-CONF

Measurement of the W helicity in $t\bar{t}$ decays at $\sqrt{s} = 1.96$ TeV in the Lepton+jets Final States using a Lifetime Tag

The DØ Collaboration

Version 0.7
URL http://www-d0.fnal.gov
(Dated: August 6, 2004)

A measurement of the W-helicity in $t\bar{t}$ decays at $\sqrt{s} = 1.96$ TeV has been carried out using data collected by the DØ detector. Semileptonic $t\bar{t}$ events in the electron and muon channel with b-jets identified by secondary vertices were used. In these events the distribution of the angle between the lepton and the direction of the intermediate W boson measured in its restframe is sensitive to the helicities of the W. With an integrated luminosity of 168.7 pb^{-1} and 158.4 pb^{-1} in the e+jets and μ+jets channels respectively, an upper limit on the fraction f_+ of positive helicity W's of $f_+ < 0.244$ is set at 90% confidence level.

Preliminary Results for Summer 2004 Conferences

I. INTRODUCTION

The fact that the top quark is so massive has led to speculations that its interactions might be especially sensitive to new physics that might appear at the TeV energy scale. In the Standard Model the decay of the top quark is described by the V-A charged current interaction. The distribution of the down-type decay products (charged lepton or d,s quark) in the rest frame of the W has the general form [1]:

$$\omega(\theta) = \frac{4}{3}\left(m_t^2\omega_0(\theta) + 2M_W^2\omega_-(\theta) + m_b^2\omega_+(\theta)\right) \ , \tag{1}$$

where θ refers to the decay angle of the down-type particle in the W restframe as shown in Figure 1. The normalized angular functions $\omega_i(\theta)$ $(i = 0, -, +)$ are:

$$\omega_0(\theta) \ = \ \frac{3}{4}\sin^2\theta \ , \tag{2}$$

$$\omega_-(\theta) \ = \ \frac{3}{8}(1-\cos\theta)^2 \ , \tag{3}$$

$$\omega_+(\theta) \ = \ \frac{3}{8}(1+\cos\theta)^2 \ . \tag{4}$$

These functions reflect the angular helicity states of the W. Introducing the helicity fractions $f_i(i = 0, -, +)$, Eq. (1) can be written in the form:

$$\tilde{\omega}(\theta) = \frac{\omega(\theta)}{\frac{4}{3}(m_t^2 + 2M_W^2 + m_b^2)} = f_0\omega_0(\theta) + f_-\omega_-(\theta) + f_+\omega_+(\theta) \tag{5}$$

These fractions depend on m_t, M_W and m_b and correspond to the branching fractions of $t \to bW$, with W in longitudinal, left-handed, and right-handed helicity states, respectively.

The fraction of longitudinal polarized W's is predicted to be

$$f_0 = \frac{m_t^2}{2M_W^2 + m_t^2 + m_b^2} = (70.1 \pm 1.6)\,\% \tag{6}$$

and f_+ is suppressed by chiral factors of order m_b^2/m_t^2. In this analysis the parameter f_0 is fixed to this predicted value.

In scenarios where the top has also a V+A charged current interaction the fraction of longitudinally polarized W's is unchanged, while the fraction of left handed W's is reduced in favor of right handed W's. A measurement of the W helicity can therefore probe the underlying weak interaction of the top decay. A next to leading order (NLO) calculation already shows that a value of $f_+ \geq 0.01$ must originate from non-SM physics [2].

The parameters f_0 and f_+ have already been measured by CDF and DØ in Run I of the Tevatron. CDF measured $f_0 = 0.91 \pm 0.37 \pm 0.13$ and $f_+ = 0.11 \pm 0.15$ [3] and DØ measured $f_0 = 0.56 \pm 0.31$ [4].

The decay of the W boson into quarks is not analyzed here, as it is experimentally very difficult to distinguish down-type quarks from up-type quarks in the W decay. The analysis presented here is carried out only for the W boson decaying into a muon and a neutrino. The companion analysis in the electron channel is in progress.

II. DATA SETS

The data sample consists of 168.7 pb^{-1} in the e+jets and 158.4 pb^{-1} in the μ+jets channel from the Run II of the Tevatron.

All signal and background processes are generated at $\sqrt{s} = 1.96$ TeV. The hard interaction was simulated with ALPGEN [5]. The parton shower,hadronisation and hadron decays were simulated using PYTHIA [6]. The signal Monte Carlo consists of seven $t\bar{t}$ samples generated with different values of f_+ ranging from $f_+ = 0$ up to $f_+ = 0.3$ in steps of 0.05.

All events are processed through a full detector simulation providing tracking hits, calorimeter cell energy and muon hit information. Extra interactions are added to all events subject to Poisson statistics given the instantaneous luminosities typically observed in the run. The same reconstruction is applied to data and Monte Carlo events.

When using simulated samples for analysis, additional smearing of the momenta of muons, electrons and jets is performed according to the observed resolutions in data.

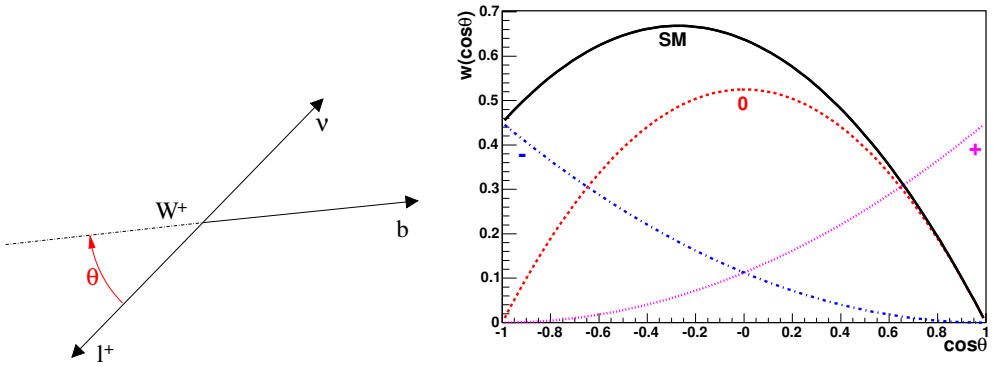

FIG. 1: Definition of the decay angle θ in the W restframe (left): θ is the angle between the down-type particle from the W decay (lepton or d,s quark) and the original W momentum. The right plot shows the angular functions $\omega(\cos\theta)$ for the three different helicity states of the W. The solid line shows the prediction of the Standard Model

III. OBJECT IDENTIFICATION

The DØ detector is a large, multipurpose collider detector with a central tracking volume immersed in a 2 T solenoidal magnetic field, surrounded by a Uranium/LAr sampling calorimeter, and located inside a full coverage muon detector. These detectors provide excellent capabilities for the identification and measurement of electrons, jets, muons and neutrinos.

Electrons are identified as clusters in the electromagnetic layers of the calorimeter found within $\Delta R \equiv \sqrt{(\Delta\phi)^2 + (\Delta\eta)^2} = 0.2$ using the simple cone algorithm. These clusters are further required to be isolated from nearby hadronic energy, to satisfy a loose shower shape selection, and to satisfy a loose match to a central track. In the final selection a multiparameter likelihood discriminant is used which compares the probabilities of a particular candidate to be an electron or background (i.e. a highly electromagnetic jet), $\mathcal{L}_e = \prod \frac{p_{S,i}}{p_{S,i}+p_{B,i}}$, where $p_{S,i}$ and $p_{B,i}$ are the probabilities to be signal or background, respectively, given a measurement i. This likelihood is constructed from the distributions in data of the electromagnetic energy fraction, shower shape, spatial track match, E/p, distance of closest approach of the track to the primary vertex, and two tracking isolation variables (one in a narrow cone, and one in a wide cone). Both central ($|\eta| < 1.1$) and forward ($1.5 < |\eta| < 2.5$) electrons are utilized for the analyses. Energy scale corrections are derived from observing electrons from Z decays and using the known Z mass as a constraint.

Muons are comprised of a track segment in the inner muon layer matching a segment formed from hits in the outer two muon layers. A central track must also match the muon track, and the overall track $\chi^2_{track} < 4$. Timing cuts are applied based on muon scintillator signals which reject cosmic ray muons. All muons must be found in $|\eta| < 2.0$. Muons supposedly originating from W (or Z) decay are identified using two isolation criteria: energy deposition near the muon as measured in the calorimeter, and an analogous measure as observed in the central tracker. The significance of the distance of closest approach of the muon track from the primary event vertex ($|dca|/\sigma_{dca}$) is required to be small, i.e. non-indicative of a heavy flavor decay muon.

Jets are reconstructed using an iterative algorithm integrating energy observed in the calorimeter in a cone with radius, $\Delta R = 0.5$. These jets are required to be in the region $|\eta| < 2.5$. Cuts on the longitudinal energy deposition profile and the energy fraction of the leading cell are applied which efficiently discriminate between real jets and those arising from hot calorimeter cells. The energy of jets is corrected after reconstruction based on studies of response (R), showering (S), and underlying event, extra interactions and noise (O) according to $E = \frac{E^{meas} - O}{R*S}$. These corrections bring the jet energy scale to the level of the particles that are incident on the calorimeter inner wall. An equivalent correction is derived for Monte Carlo events to bring them to the same level as the data. A further correction for b-jets is applied when a soft muon is found in a jet. This correction compensates for all of the muon energy, and all of its corresponding neutrino energy to be unobserved in the calorimeter.

A global event quantity, termed missing transverse energy, or $\not\!\!E_T$, is calculated to give an indication of neutrinos of substantial P_T in an event. The transverse energy in the calorimeter towers is vectorially summed. The missing E_T is then the negative of this sum and implies an unmeasured imbalance in the event due to a neutrino. The outer, coarse hadronic layer of the calorimeter is omitted in this sum, unless such energy comprises a reconstructed jet. The change in each electron or jet P_T due to response corrections as described above is vectorially added into the $\not\!\!E_T$, as

are any observed muons.

The event primary vertex is calculated from reconstructed central tracks. Events are rejected if this vertex is not found to be within $|z| < 60.0$ cm of the center of the detector, or if it is not calculated from at least 3 tracks.

A. b-tag

One of the main ingredients for this analysis is the usage of secondary vertex information to identify heavy flavor jets, allowing a further background reduction.

The algorithm consists of three main steps:

- reconstruction of the primary vertex,
- reconstruction of track-based jets and
- reconstruction of secondary vertices within these jets.

A jet is defined to be tagged if it contains a secondary vertex which is displaced by more than seven standard deviations from the primary vertex. The tagging efficiency for b and c quarks as well as the mistag efficiency for light quarks is parametrized as a function of jet E_T and η. These parametrizations are then applied to the $t\bar{t}$ and the W+jets Monte Carlo samples.

IV. EVENT PRESELECTION

The event preselection in the e+jets and the μ+jets channel requires

- an electron or isolated muon with $p_T > 20$ GeV,
- no second lepton with $p_T > 15$ GeV in the event,
- high transverse missing energy : $\not\!\!E_T > 17$ GeV (μ+jets) or $\not\!\!E_T > 20$ GeV (e+jets),
- at least four jets with $p_T > 15$ GeV and $|\eta| < 2.5$,
- at least one jet tagged by the secondary vertex tagging algorithm,
- a converged kinematic fit as described in Section VI.

After these preselection cuts 14 events remain in the μ+jets channel and 33 events in the e+jets channel.

V. SIGNAL-TO-BACKGROUND DISCRIMINATION

The two main backgrounds to $t\bar{t}$ pair production in the lepton+jets channel arise from the W multijet production and from QCD multijet events in which one jet fakes a isolated muon or electron.

A. Estimation of QCD background

The QCD background is estimated using data: Two samples of events, a loose and a tight set, are selected, the latter being a subset of the first. The efficiency of the tight selection is higher for isolated leptons from W+jets and $t\bar{t}$ events than from leptons from b-quark decays in the QCD background. This difference can then be used to extract the expected number of QCD events in the tight sample.

B. Discrimination of W+jets background

To discriminate between W multijet production and $t\bar{t}$ pair production, a likelihood discriminant is built using the following variables:

Sphericity: the normalized momentum tensor $\mathcal{M}$ is defined as:

$$\mathcal{M}_{ij} = \frac{\Sigma_o p_i^o p_j^o}{\Sigma_o |\vec{p^o}|^2}, \tag{7}$$

where $\vec{p^o}$ is the momentum-vector of a reconstructed object o, i and j are Cartesian coordinates. The objects included in the sum are the jets and the lepton from the W decay, which have the best discrimination power between $t\bar{t}$ and W+jets. By standard diagonalization of $\mathcal{M}_{ij}$, three eigenvalues $\lambda_1 \geq \lambda_2 \geq \lambda_3$ are found, with $\lambda_1 + \lambda_2 + \lambda_3 = 1$. The sphericity of the event is then defined as

$$S = \frac{3}{2}(\lambda_2 + \lambda_3), \tag{8}$$

so that $0 \leq S \leq 1$. Sphericity is essentially a measure of the summed $p_\perp^2$ with respect to the event axis; a 2-jet event corresponds to $S \approx 0$ and an isotropic event to $S \approx 1$. $t\bar{t}$ events are quite isotropic as is typical for the decay of a heavy object. W+jets and QCD events are less isotropic, primarily due to the fact that the jets in these events arise from initial and final state radiation.

Aplanarity: the aplanarity $\mathcal{A}$, a measure of the flatness of the event, is defined as $\mathcal{A} = \frac{3}{2}\lambda_3$, where λ_3 is the smallest eigenvalue of the normalized momentum tensor $\mathcal{M}$ (see Eq. (7)). Therefore, it is defined in the range $0 \leq \mathcal{A} \leq 0.5$. Large values of $\mathcal{A}$ are an indication of spherical events, whereas small values correspond to more planar events. $t\bar{t}$ events are quite spherical as is typical for the decay of a heavy object. W+jets and QCD events are more planar, primarily due to the fact that the jets in these events arise from initial and final state radiation.

Centrality: the centrality C is defined as

$$C = \frac{H_T}{H_E} = \frac{\sum_{jet=1}^{N_{jets}} E_T(jet)}{\sum_{jet=1}^{N_{jets}} E(jet)}, \tag{9}$$

where H_T is the sum of the transverse jet energies and H_E is the total jet energy in the event. It provides a handle on what fraction of the energy deposited in the proton-antiproton collision is transverse energy.

H_T^3: is defined as

$$H_T^3 = H_T - E_T(jet1) - E_T(jet2), \tag{10}$$

where $jet1$ and $jet2$ are the leading and second-leading jet, respectively.

M_{min}: the smallest invariant mass of any two jets in the event.

HitFit χ^2: the χ^2 from the kinematic fit described in Section VI provides a measure on how *top-like* the event is.

Only the four leading jets are used to determine these variables. This does not reduce the statistical separation power but it reduces the dependence on systematic effects from the modeling of soft radiation (e.g. underlying event). The likelihood output $\mathcal{L}$ is given by

$$\mathcal{L} = \frac{\exp\left(\sum_i (\ln \frac{S}{B})^i_{\text{fitted}}\right)}{\exp\left(\sum_i (\ln \frac{S}{B})^i_{\text{fitted}}\right) + 1}, \tag{11}$$

where $(\ln \frac{S}{B})^i_{\text{fitted}}$ is the fit to $\ln(\frac{\mathcal{P}^i_{\text{t}\bar{\text{t}}}}{\mathcal{P}^i_{\text{W}}})$ for each variable i that is used to build the discriminant, and $\mathcal{P}^i_{\text{t}\bar{\text{t}}}$ and $\mathcal{P}^i_{\text{W}}$ are the probabilities for the variable i to be $t\bar{t}$ signal and $W + jets$ background, respectively.

Tables I list the correlations between the input variables of the likelihood discriminant and the decay angle $\cos\theta$. None of the input variables shows a strong correlation with $\cos\theta$. The likelihood discriminant has been derived separately for the muon and for the electron channel after all preselection cuts and after applying the b-tag.

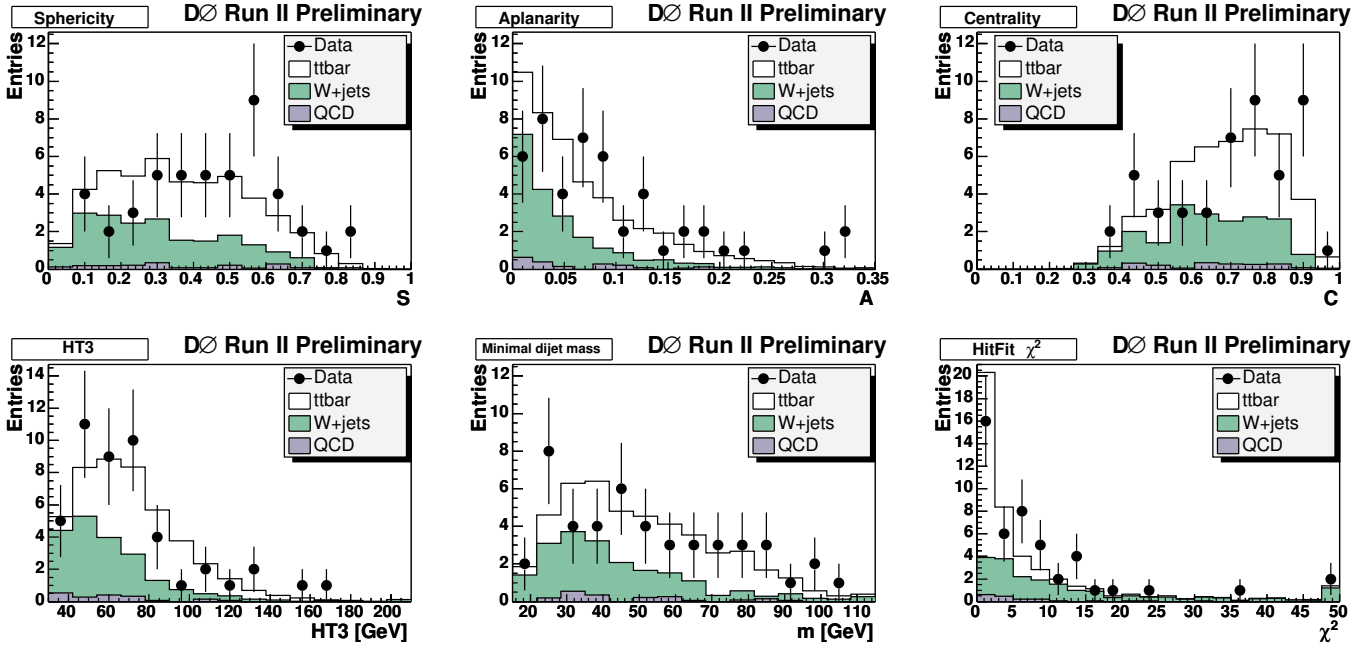

FIG. 2: Input variables for the likelihood discriminant after all preselection cuts and after applying the b-tag. From top left to bottom right: sphericity, aplanarity, centrality, H_T^3, minimal dijet mass and the χ^2 from the kinematic fit. Both channels are combined in these plots.

Variable	Centrality	Aplanarity	H_T^3	Sphericity	M_{min}	χ^2	$\cos\theta$
Centrality	1.000	0.177	0.158	0.177	-0.025	-0.009	-0.032
Aplanarity	0.156	1.000	0.164	0.635	0.105	-0.085	0.009
H_T^3	0.166	0.125	1.000	0.085	0.521	0.040	0.094
Sphericity	0.153	0.639	0.053	1.000	0.043	-0.101	0.012
M_{min}	0.002	0.105	0.521	0.033	1.000	-0.009	0.074
χ^2	-0.033	-0.088	0.097	-0.099	-0.023	1.000	0.178
$\cos\theta$	-0.071	0.041	0.112	0.029	0.089	0.079	1.000

TABLE I: Correlation between the input variables for the Likelihood discriminant and the decay angle $\cos\theta$. Values above the diagonal are derived in the μ+jets channel, whereas the ones below the diagonal correspond to the e+jets channel.

VI. RECONSTRUCTION OF THE TOP QUARK

The top quarks are reconstructed using a kinematic fit. This fit is performed by minimizing a χ^2 defined as

$$\chi^2 = (\vec{x} - \vec{x}_M)G(\vec{x} - \vec{x}_M)^T \ , \tag{12}$$

where $\vec{x}_M$ is a vector of measured variables, $\vec{x}$ is a vector of fitted variables and G is the inverse error matrix of the measured quantities. The minimization is subject to the following constraints:

- two jets must form the invariant mass of the W,
- the lepton and the missing transverse energy must form the invariant mass of the W,
- the masses of the two reconstructed top quarks must be equal.

Up to this point the usage of the kinematic fit is the same as for the top mass measurement. Since this analysis is not targeted at measuring the top mass, it is possible to also constrain the top mass to be 175 GeV. The mass constraint improves the resolution of the reconstructed decay angle by 10%.

Without any knowledge about the jets, there are 12 possible jet permutations. The b-tag information is not used to reduce the number of possible permutations. Among the possible combinations the one with the lowest χ^2 is chosen.

VII. MEASUREMENT OF THE W HELICITY

The normalization of the signal and background templates is derived by performing a likelihood fit to the likelihood discriminant from Section V B. A cut on the likelihood discriminant is then applied to further reduce the background.

Due to resolution and reconstruction effects it is not possible to directly fit the measured decay angle distribution with the theoretical prediction and obtain the fraction of right handed W's. Therefore templates of the decay angle $\cos\theta$ for different values of f_+ and for the background are compared to the data.

A. Final selection

The number of $t\bar{t}$ events in the selected data sample can directly be extracted by performing a likelihood fit to the likelihood discriminant. Since the relative fractions of W+jets and $t\bar{t}$ events is already known from the estimation of the QCD background a likelihood $\mathcal{L}$ can be constructed containing this constraint. This is realized by defining the likelihood as follows:

$$\mathcal{L}(N_{t\bar{t}}, N_W, N_{\rm QCD}) = \prod_i P(n_i^{\rm obs}, \nu_i) \ \cdot \ P(N_{\ell-t}^{\rm obs}, N_{\ell-t}) \tag{13}$$

where $P(n,\nu)$ generically denotes the Poisson probability density function for n observed events given an expectation of ν. The product in the first term of Eq. (13) runs over all bins, i, in the Likelihood discriminant. The second term of Eq. (13) is a Poisson constraint on the observed number of events in the loose sample minus the number of events in the tight sample, $N_{\ell-t}^{\rm obs} = N_\ell - N_t$. $N_{\ell-t}$ is the predicted number of events in the "loose-tight" sample.

Figure 3 shows the distribution obtained in data of the likelihood discriminant after all preselection cuts.

The result from this fit is summarized in Table II.

Channel	$t\bar{t}$	W+jets	QCD
μ+jets	10.2 ± 2.9	3.1 ± 2.2	0.9 ± 0.2
e+jets	16.9 ± 4.1	14.9 ± 4.0	1.0 ± 0.3

TABLE II: Fitted number of events for the three different samples in each of the two channels.

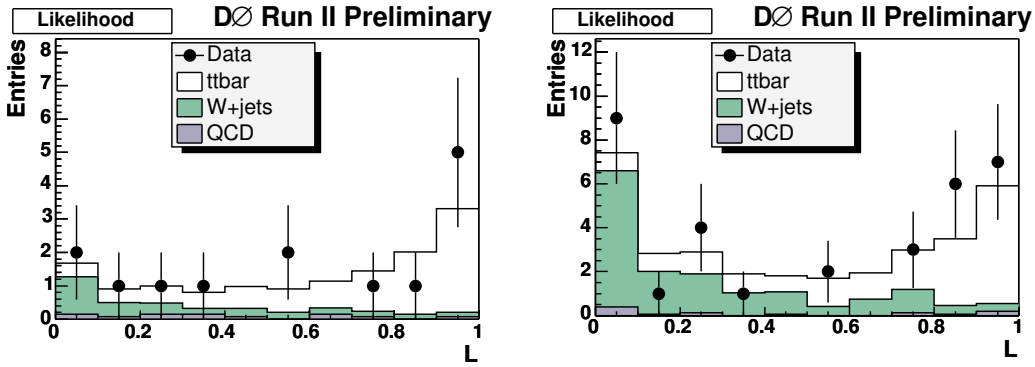

FIG. 3: Likelihood discriminant after all preselection cuts in the muon channel (left) and the electron channel (right). All Monte Carlo samples are normalized to the result from the Fit to the likelihood discriminant.

To further reduce the background, a cut on the likelihood discriminant is applied. This cut is optimized to maximize the statistical significance between the V+A and the V-A scenarios. The significance is here defined to be

$$S = \sum_{i=1}^{N_{bins}} \frac{(n_{i,V-A} - n_{i,V+A})^2}{n_{i,V-A} + n_{i,V+A}}, \tag{14}$$

where the sum runs over all bins in the decay angle histogram and n_i is the content of bin i after adding up signal and background.

The optimal cut is found to be at $\mathcal{L} \geq 0.1$ in the muon channel and at $\mathcal{L} \geq 0.3$ in the electron channel. This cut does not distort the shape of the $\cos\theta$ distribution. The Monte Carlo normalization after this cut is based on the numbers obtained from the fit to the likelihood discriminant and the efficiencies of this cut. Table III summarizes the predicted number of events for each sample.

Channel	$t\bar{t}$	W+jets	QCD
μ+jets	9.6 ± 2.7	2.0 ± 1.4	0.7 ± 0.4
e+jets	14.2 ± 3.4	6.6 ± 1.8	0.6 ± 0.3

TABLE III: Predicted number of events for the three different samples in each of the two channels after the cut on the likelihood discriminant.

B. Templates

The decay angle templates for the signal and the W+jets background sample are taken from Monte Carlo, while the template for the QCD background is derived from the tagged data, by reversing the tight criteria for the isolation in the muon channel and for the electron likelihood in the electron channel.

The 7 different signal templates have a sizable statistical uncertainty. To reduce this uncertainty the 7 templates are interpolated to create just two templates: a template for V-A and a template for V+A. This is possible, because the interference Term between V-A and V+A is negligible and therefore all f_+ fractions can be reproduced by a linear combination of the V-A and the V+A template.

The templates are interpolated in the following way:

- for each of the 7 Monte Carlo signal samples the decay angle distribution is plotted into a histogram;
- the content of each bin i of these histograms is plotted against the corresponding V+A fraction;
- the resulting graph is fitted with a straight line;
- the templates for V-A and for V+A are created using the parameters and uncertainties from the fit.

C. Limit calculation

A binned maximum likelihood fit is used to extract the value of f_+ using the decay angle templates for the QCD and the W+jets background and the interpolated signal templates. The likelihood is built by multiplying the Poisson probabilities of each template bin:

$$\mathcal{L}(f_+) = \prod_{i=1}^{N_{bins}} (\mu_i(f_+) + b_i)^{n_i} \cdot \frac{\exp[-(\mu_i(f_+) + b_i)]}{n_i!} \,, \tag{15}$$

where n_i is the number of data events in the ith data bin, b_i is the predicted background contribution and $\mu_i(f_+)$ is the predicted signal contribution given the f_+ value.

For each value of f_+ the negative logarithm of the likelihood is calculated. The resulting distribution of $-\ln\mathcal{L}$ points versus f_+ is fitted with a parabola to get the likelihood as a function of f_+. Due to the interpolation of the signal templates these $-\ln\mathcal{L}$ are correlated and all points lie on the parabola.

A Bayesian technique is now used to determine a confidence interval with a given confidence level (C.L.) β for the true value of f_+. Since f_+ is restricted to values between 0 and 0.3, the following prior is used:

$$\pi(f_+) = \begin{cases} 1 & 0 \leq f_+ \leq 0.3 \\ 0 & f_+ < 0 \text{ or } f_+ > 0.3 \end{cases} \tag{16}$$

In case the maximum of the likelihood is outside the physically allowed range (or close enough to the boundary that the 1σ error is partially in the unphysical region), an upper limit x_{upper}

$$\frac{\int_{-\infty}^{x_{upper}} \pi(x)\mathcal{L}(x)\,\mathrm{d}x}{\int_{-\infty}^{\infty} \pi(x)\mathcal{L}(x)\,\mathrm{d}x} = \frac{\int_{0}^{x_{upper}} \mathcal{L}(x)\,\mathrm{d}x}{\int_{0}^{0.3} \mathcal{L}(x)\,\mathrm{d}x} = \beta \tag{17}$$

or a lower limit x_{lower}

$$\frac{\int_{x_{lower}}^{\infty} \pi(x)\mathcal{L}(x)\,\mathrm{d}x}{\int_{-\infty}^{\infty} \pi(x)\mathcal{L}(x)\,\mathrm{d}x} = \frac{\int_{x_{lower}}^{0.3} \mathcal{L}(x)\,\mathrm{d}x}{\int_{0}^{0.3} \mathcal{L}(x)\,\mathrm{d}x} = \beta \tag{18}$$

is reported with the confidence level β.

VIII. SYSTEMATICS

The presented analysis relies on shapes and not on overall normalizations. The dominant systematic uncertainties are therefore the ones which potentially change the shape of the distributions.

The following systematic effects have been studied:

Uncertainty associated to the top quark mass The mass of the top quark enters into the kinematic fit as a constraint ($m_{top} = 175$ GeV). To study the systematic effect due to this constraint, signal templates with $m_{\mathrm{top}} = 170$ GeV and $m_{\mathrm{top}} = 180$ GeV, respectively, have been used.

Uncertainty associated to the jet energy scale (JES) The effect of the jet energy scale uncertainty on the shape of the decay angle distribution is obtained by varying the JES by one standard deviation, where, conservatively,

$$\Delta = \sqrt{\Delta^2_{stat,data} + \Delta^2_{syst,data} + \Delta^2_{stat,MC} + \Delta^2_{syst,MC}}. \tag{19}$$

The individual terms are the statistical and systematic uncertainties on the JES in data and in Monte Carlo.

Uncertainty associated to the limited MC statistics The decay angle templates used in this analysis have a sizable statistical uncertainty which in the case of the signal templates could be reduced by interpolation. These uncertainties have been taken into account.

Uncertainty associated with the underlying event in the MC In all W+jets Monte Carlo samples the underlying event was switched off. To estimate this effect the change in shape due to the underlying event has been applied to all W+jets Monte Carlo samples.

Uncertainty associated with the fit to the likelihood discriminant The uncertainties on the number of signal, W+jets and QCD events from the fit are treated as systematic uncertainties. The anti-correlation between the number of W+jets and signal events was taken into account.

Uncertainty associated with the flavor composition of the W+jets background The exact flavor composition of the W+jets background is not known and can only estimated using the relative theoretical cross-section, the jet-parton matching and the parametrized b-tagging efficiency. To get a handle on the size of this effect, the predicted W+jets flavor composition has been replaced by events with only light quarks and by events with two b quarks.

The Bayesian limit calculation takes the systematic uncertainties into account by convoluting a Gaussian function with a width given by the total systematic uncertainty with the likelihood.

The magnitude of each systematic uncertainty is estimated by running ensemble tests. The templates used to analyze each toy experiment are the standard templates while the toy experiments are created using the varied templates.

In order to reduce the sensitivity to statistical fluctuations inside these ensemble tests, the number of events in the ensemble is increased by a factor of 100.

The individual systematic effects are added in quadrature to obtain the total systematic uncertainty summarized in Table IV.

Source	Uncertainty
Jet energy scale	0.065
Underlying Event	0.063
Top mass	0.060
Likelihood Fit (muon channel)	0.020
Likelihood Fit (electron channel)	0.014
Composition of W+jets background	0.012
Monte Carlo statistics	0.012
Total	0.112

TABLE IV: Summary of systematic errors on f_+.

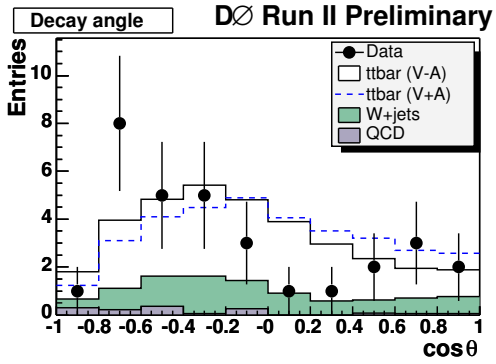

FIG. 4: Decay angle distribution after all selection cuts. Both channels are combined. The V-A, i.e. $f_+ = 0.00$, as well as the V+A, i.e. $f_+ = 0.30$, $t\bar{t}$ Monte Carlo is shown. The different Monte Carlo samples have been normalized to the expected number of events estimated using the result from the likelihood fit and the efficiencies of the likelihood cut.

IX. ENSEMBLE TESTS

To test the performance of this analysis, Monte Carlo ensemble tests have been performed. In these tests f_+ is set to 0.00. The Monte Carlo experiments are created by taking the predicted number of events from the fit to the likelihood discriminant and the efficiencies of the cut on the discriminant. For each bin in the decay angle histogram and for each sample (QCD, W+jets and $t\bar{t}$) a Poisson process is assumed to obtain the number of events in this bin.

The obtained decay angle distribution is then analyzed. By repeating this process a large number of times, a distribution for the limit at 90% confidence level has been obtained. The mean of this distributions corresponds to the expected limit at 90% C.L.: 0.253.

X. RESULT

After all selection cuts 12 events remain in the muon channel and 19 events in the electron channel. Their combined decay angle distribution is shown in Figure 4.

The extracted value of f_+ from the fit to the $-\ln\mathcal{L}(f_+)$ points shown in Figure 5 is

$$f_+ = -0.13 \pm 0.23\ (stat). \tag{20}$$

This fit is not restricted to the physically allowed region.

The corresponding Bayesian limit calculation, which includes the bound of the physically allowed region, yields the following result:

$$f_+ < 0.244\ \ (90\%\ \text{C.L.}). \tag{21}$$

A frequentist analysis based on the prescription given by Feldman&Cousins [7] has also been performed which returns a similar result.

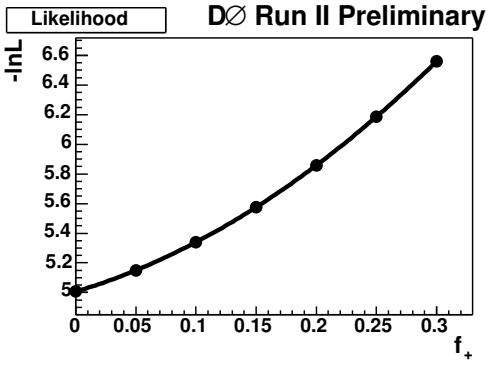

FIG. 5: Result of the maximum likelihood fit. The fact that all likelihood points lie perfectly on the fitted parabola is due to the interpolation of the templates.

XI. SUMMARY

A measurement of the f_+, the fraction of W's with positive helicity from the top decay, in the ℓ+jets channel using Run II data has been presented. The datasets used in this analysis correspond to an integrated luminosity of 158.4 pb^{-1} in the μ+jets channel and 168.7 pb^{-1} in the e+jets channel. After selection and application of a Secondary Vertex tag, a kinematic fit to the $t\bar{t}$ hypothesis is performed and an event discriminant between signal and background is built. A Bayesian limit calculation is performed yielding the following upper limit on f_+ with 90% confidence:

$$f_+ < 0.244 \ \ (90\% \text{ C.L.})$$

A frequentist analysis based on the prescription given by Feldman&Cousins has also be performed which returns a similar result.

XII. ACKNOWLEDGMENTS

We thank the staffs at Fermilab and collaborating institutions, and acknowledge support from the Department of Energy and National Science Foundation (USA), Commissariat à l'Energie Atomique and CNRS/Institut National de Physique Nucléaire et de Physique des Particules (France), Ministry of Education and Science, Agency for Atomic Energy and RF President Grants Program (Russia), CAPES, CNPq, FAPERJ, FAPESP and FUNDUNESP (Brazil), Departments of Atomic Energy and Science and Technology (India), Colciencias (Colombia), CONACyT (Mexico), KRF (Korea), CONICET and UBACyT (Argentina), The Foundation for Fundamental Research on Matter (The Netherlands), PPARC (United Kingdom), Ministry of Education (Czech Republic), Natural Sciences and Engineering Research Council and WestGrid Project (Canada), BMBF (Germany), A.P. Sloan Foundation, Civilian Research and Development Foundation, Research Corporation, Texas Advanced Research Program, and the Alexander von Humboldt Foundation.

[1] R. H. Dalitz and G. R. Goldstein, "The Decay And Polarization Properties Of The Top Quark," Phys. Rev. D **45**, 1531 (1992).
[2] H. S. Do, S. Groote, J. G. Korner and M. C. Mauser, "Electroweak and finite width corrections to top quark decays into transverse and longitudinal W-bosons," Phys. Rev. D **67**, 091501 (2003) [arXiv:hep-ph/0209185].
[3] T. Affolder *et al.* [CDF Collaboration], "Measurement of the helicity of W bosons in top quark decays," Phys. Rev. Lett. **84**, 216 (2000) [arXiv:hep-ex/9909042].
[4] F. Canelli, "Helicity of the W in Single-Lepton ttbar Events", PhD Thesis, University of Rochester, 2003 D0 Collaboration, hep-ex/0404040 (2004).
[5] M. L. Mangano, M. Moretti, F. Piccinini, R. Pittau and A. D. Polosa, "ALPGEN, a generator for hard multiparton processes in hadronic collisions," JHEP **0307**, 001 (2003) [arXiv:hep-ph/0206293].
[6] T. Sjostrand, L. Lonnblad and S. Mrenna, "PYTHIA 6.2: Physics and manual," arXiv:hep-ph/0108264.
[7] G. J. Feldman and R. D. Cousins, "A Unified approach to the classical statistical analysis of small signals," Phys. Rev. D **57**, 3873 (1998) [arXiv:physics/9711021].